Phosphorus Nanostructures

DOI: 10.1002/ange.200805222

Synthesis of Pure Phosphorus Nanostructures**

*Richard A. L. Winchester, Max Whitby, and Milo S. P. Shaffer**

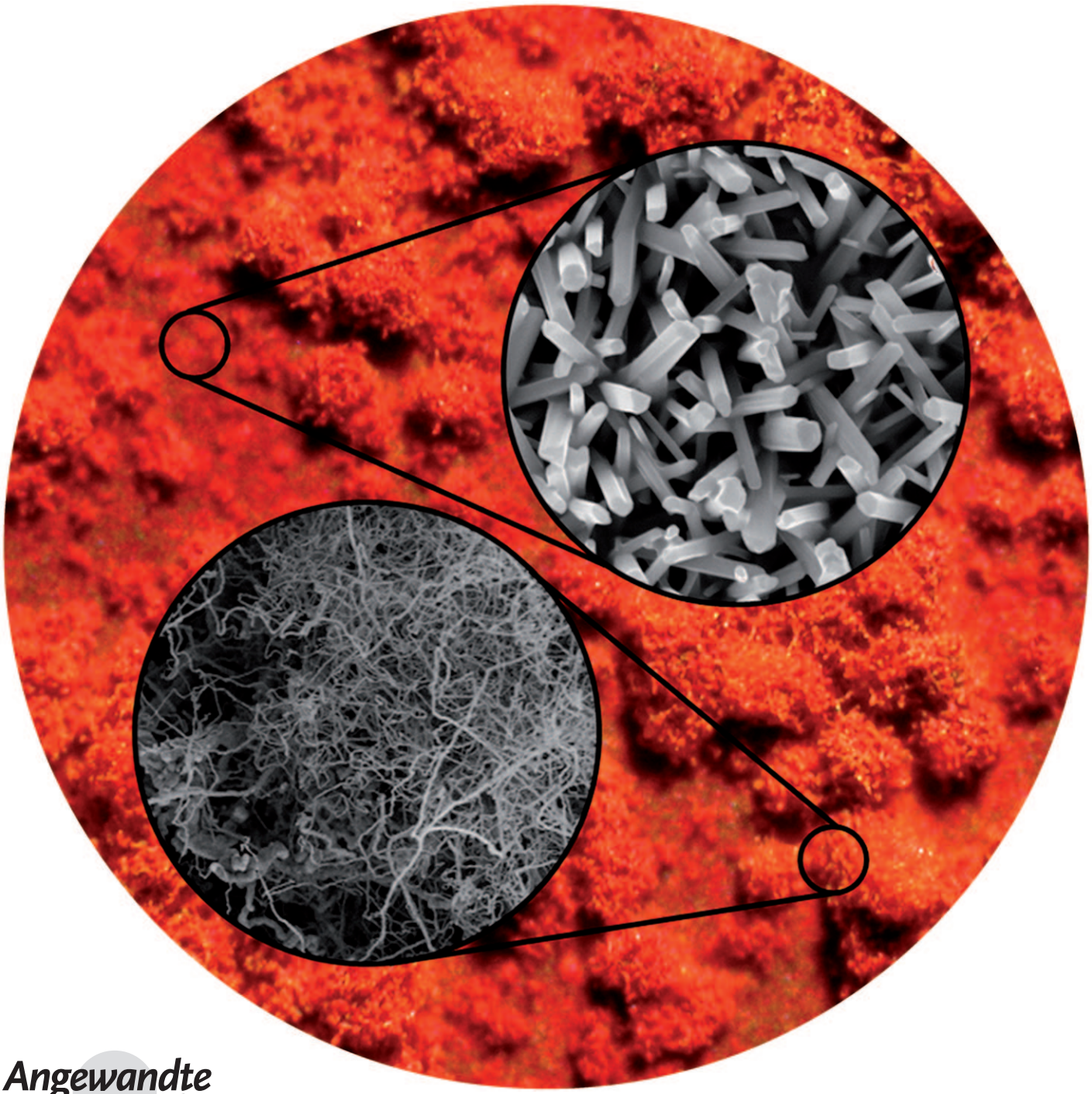

Elemental phosphorus is known to exist as several different allotropes, commonly referred to as white, red, and black phosphorus, after their various colors. Although the white and black allotropes have been well characterized,[1,2] the evidence concerning the numerous red allotropes of phosphorus is less comprehensive.[3] Amorphous red phosphorus is formed by exposing white phosphorus to heat, light, or X-rays.[4] Heating amorphous red phosphorus yields different crystalline polytypes depending on the conditions. In a previous study, Roth et al.[5] proposed the existence of five distinct red allotropes, based on optical microscopy, differential thermal analysis (DTA), and powder X-ray diffraction. Commercially-available amorphous red phosphorus was labeled as "type I", and annealed at temperatures up to 550 °C to form four other allotropes, named type II, III, IV, and V red phosphorus.[5] Little is known about types II and III, as a result of the difficulty of growing crystals suitable for single-crystal X-ray diffraction. Type IV is often referred to as fibrous red phosphorus and its structure has recently been determined.[6] Type V is more often referred to as Hittorf's phosphorus, named after its discoverer in 1865.[7] Both fibrous and Hittorf's phosphorus are formed from complex polymeric pentagonally linked rings, connected in differing orientations, with the repeating unit, in each case, consisting of 21 phosphorus atoms. Theoretical studies by Haser and Bocker[8] suggest that a variety of other repeating units show similar stability and may be present in type II or III red phosphorus. The structure of polymeric phosphorus strands found in CuI matrices supports this theoretical work.[9] Recently, two new allotropes of phosphorus, based on repeating P_{12} units, were isolated from CuI.[10] The authors named these phosphorus strands "nanorods", although they are more polymeric in character, with a radius of only 3–5 Å. Further calculations suggest that icosahedral and ring-shaped allotropes of phosphorus may also be viable.[11]

Herein, we demonstrate the possibility of rationally growing high aspect ratio nanostructures of pure phosphorus. Research into high aspect ratio nanostructures, such as nanotubes, nanowires, and nanorods, has been driven forward recently by both fundamental science and applications ranging from nanoelectronics[12] to composites.[13] The synthesis of isolated, pure, phosphorus structures of this type has, to our knowledge, not been reported to date. Theoretical studies suggest that single-wall phosphorus nanotubes are stable,[14,15] although the selection of rhombohedral black phosphorus as the underlying motif (which is only stable at pressures over 5.5 GPa, unlike the more common orthorhombic form[16]) may limit the practical relevance of these calculations. Nevertheless, the possibility of phosphorus nanorods and nanotubes is worthy of experimental investigation, and provides insight into phosphorus allotropy in general.

The vapor–liquid–solid (VLS) mechanism is one of the most common routes for growing 1D nanostructures.[17–19] It uses a liquid (usually metal) catalyst particle to constrain decomposition or condensation of the vapor feedstock to form a high aspect ratio solid. We therefore devised a rational synthesis to encourage the VLS growth of phosphorus nanorods and nanotubes. White phosphorus (P_4) was chosen as a convenient, volatile vapor source, with bismuth as the catalyst, owing to the low but significant solubility of gaseous P_4 in liquid bismuth, as shown by Brown and Rundqvist in their synthesis of black phosphorus needles from a bismuth melt in 1965.[2] Ampoules were produced (Figure 1) and heated in a muffle furnace to temperatures in the range 300–460 °C.

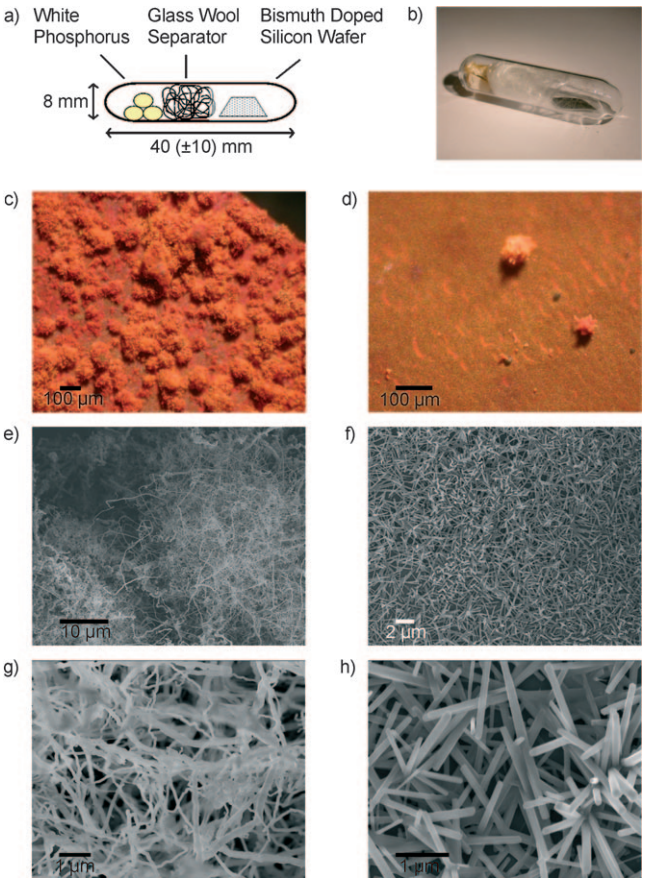

Figure 1. a) Schematic diagram and b) photograph of a typical ampoule before heat treatment; c) and d) show optical micrographs and e–h) SEM images of the mixed product, as deposited on the Si wafer during synthesis. Two components dominate: high aspect ratio "tangles" (images (c), (e), and (g)) and shorter, straighter "grass" (images (d), (f), and (h)).

[*] R. A. L. Winchester, Dr. M. S. P. Shaffer
Department of Chemistry
Imperial College London, SW7 2AZ (UK)
Fax: (+44) 20-7594-5801
E-mail: m.shaffer@imperial.ac.uk

M. Whitby
RGB Research Ltd
3 Warple Mews, London, W3 0RF (UK)

[**] We thank the EPSRC and RGB Research for financial support. We also thank Dr. Mahmoud G. Ardakani for help with electron microscopy, Richard Sweeney, Dr. Jerry Y. Y. Heng, and Johann Cho for help with X-ray diffraction, Tom Cotter for help with synthesis, and William P. Griffith for helpful discussions regarding the allotropy of phosphorus.

Supporting information for this article is available on the WWW under http://dx.doi.org/10.1002/anie.200805222.

Optical microscopy revealed that the silicon wafers from preliminary syntheses were covered in many small, red, tangled, fibrous structures (Figure 1c), between which a smoother coating of red material was deposited (Figure 1d). SEM studies show clearly that these "tangles" consist of high aspect ratio structures, a large proportion of which have diameters on the nanoscale (Figure 1e and g). Shorter, straighter one-dimensional nanostructures (referred to below as "grass" in reference to their appearance) were visible in the regions between the tangled fibers (Figure 1d, f, and h).

The tangled structures consist of polycrystalline nanorods. To investigate the relationship between the synthesis temperature and the product morphology, a set of ampoules were heated to temperatures in the range 300–460 °C for 4 h (see the Supporting Information, Section 2 for full details). Silicon wafers from these ampoules were analyzed under SEM and, although the tangled morphology makes accurate determination of the length of the nanorods impractical, their diameters were measured (Figure 2a and Supporting Information, Figure S1). The images show that a temperature of around 380 °C is optimal for the production of longer, thinner nanorods. Other temperatures yield a progressively curlier, shorter, and larger diameter product. The tangled nanorods were the major product in the range 300–420 °C, but at 460 °C they give way to a large majority of microrods or platelets (see the Supporting Information, Figure S2; details of these structures will be published separately).

High-resolution TEM images of the body of the tangled nanorods show that they are polycrystalline with common lattice spacings of around 5.7 Å (Figure 2c). This spacing strongly suggests that they consist of one of the crystalline forms of red phosphorus, however, it does not allow determination of the specific type, since all four crystalline forms have similar lattice spacings in the region of 5.6–5.9 Å, as indicated in powder diffraction studies.[5] Energy-dispersive X-ray Spectroscopy (EDS) (Figure 2c) confirms that the nanorod body consists mainly of phosphorus with only a small peak corresponding to oxygen suggesting mild surface oxidation. The polycrystalline character makes it unlikely that the high aspect ratio arises from intrinsic anisotropy of the crystal structure. TEM images (Figure 2b) show that the nanorods tips are darker than the body and EDS (Figure 2d) confirms that these globular tips consist largely of bismuth. In addition, lattice-resolved TEM of a tip structure (Figure 2d) reveals a spacing of 3.2 Å,[20] which matches the (012) plane in rhombohedral bismuth. The data strongly suggest VLS growth of polycrystalline red phosphorus nanorods from bismuth metal catalyst particles in which the diameter of the catalyst particle defines the diameter of the nanorod extruded.[17] The original pulverized bismuth particles are much larger (diameter 17 μm; see the Supporting Information, Figure S3); the active metal particles are generated in situ by vapor transport, as shown by control experiments in the absence of phosphorus (see the Supporting Information, section 4, Figure S4).

Although most VLS-grown nanostructures were found to be solid in cross-section, some TEM images suggest that tubular structures were also synthesized (Figure 3). Unfortunately, these features were extremely sensitive to the high-energy electron beam and lattice-resolved images could not be acquired. Attempts to use low dose and cryo-TEM to obtain lattice resolved images have not yet proven successful. Figure 3a shows an anisotropic structure protruding from a cluster of highly beam sensitive material. The contrast suggests that the structure is tubular and likely grew by VLS-growth from a bismuth catalyst particle at the tip.

Examination of silicon wafers from the preliminary syntheses suggested that the "grass" structures were formed

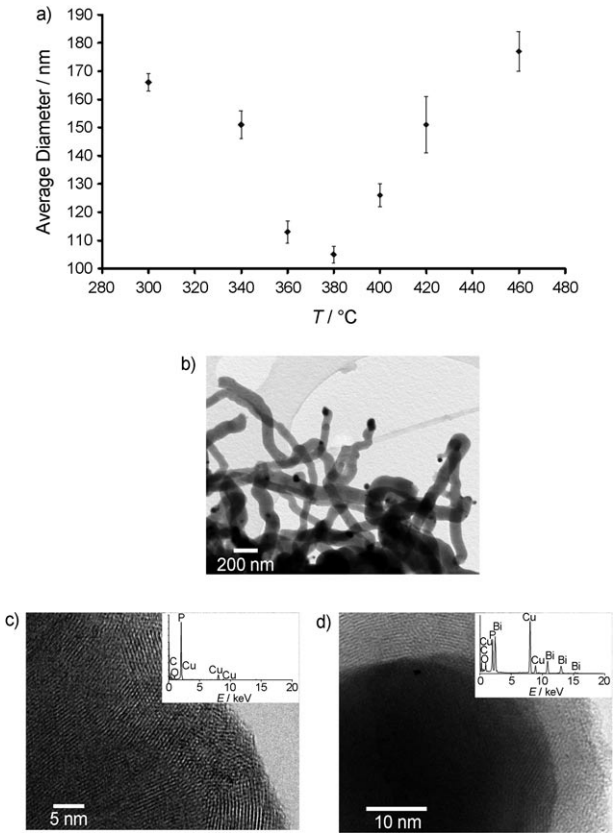

Figure 2. a) Plot of the mean nanorod diameters in the tangles as a function of synthesis temperature (mean of 100–240 rods for each data point); b–d) TEM studies of polycrystalline nanorods of which the tangles consist, showing b) the general morphology; c) and d) high-resolution images of a nanorod body and tip, respectively, with EDS spectra inset.

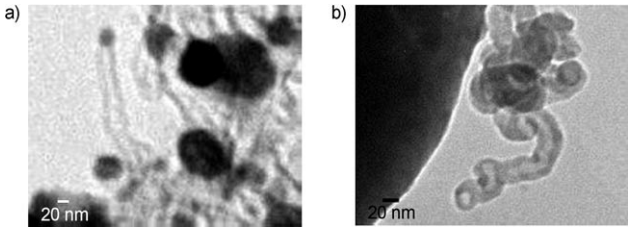

Figure 3. a, b) TEM images of beam-sensitive elongated phosphorus-containing nanostructures that appear to be hollow. Both structures melted under the electron beam within a few seconds.

in areas free of bismuth, whereas the "tangles" were formed in bismuth-rich areas. To investigate the formation of the "grass" structures, a series of ampoules containing only white phosphorus (0.06 g), a glass-wool plug, and a silicon wafer under argon were heat-treated at temperatures between 340 °C and 440 °C for 12 h. SEM images confirmed that a straight, nanorod product was formed in each case with dimensions that depended on synthesis temperature (Figure 4a). Although the lengths of the nanorods were slightly underestimated, owing to projection errors (see the Supporting Information, Figure S5), relative comparative measurements can be deduced from the data. The length and aspect ratio of the nanorods increased with temperature whereas the diameter remains unaffected.

High resolution (HR) TEM confirmed that single crystal nanorods were formed during the syntheses. Analysis of selected area electron diffraction (SAED) patterns for a selection of nanorods strongly suggested that the nanorods consist of the type II crystalline form of red phosphorus, which has not, to our knowledge, yet been fully structurally characterized. Figure 4c compares spacings obtained from powder diffraction data for type II red phosphorus[5] with the average spacings obtained by using electron diffraction from a number of nanorods. HRTEM images show spacings of 5.7 Å and 18.3 Å, parallel and perpendicular to the axis of the nanorods, respectively (Figure 4d and e). The shorter distance is consistent with the equatorial spots in the SAED pattern (●, Figure 4c). The longer spacing corresponds to the 17.9 Å feature labeled in Figure 4c. The apparent absence of meridional diffraction spots is likely a shadowing effect resulting form the thickness of the nanorods. EDS studies once again confirmed that the nanorods consist of phosphorus, with oxygen present at 10 wt%, suggesting some surface oxidation. Indeed TEM images show a thin (4 nm) coating of an amorphous substance likely to consist of phosphorus oxide, formed as a result of air exposure during TEM sample preparation (Figure 4d and e). Another possibility is that the coating consists of amorphous red phosphorus deposited during the cooling process.

Powder X-ray diffraction patterns (Figure 5a) of the products were compared to those of a range of conventional allotropes, synthesized by standard methods (see the Supporting Information, section 6). Pure type III red phosphorus has rarely, if ever, been detected, presumably owing to the apparently limited stability range relative to type II or fibrous red phosphorus.[5] Despite attempts, the published synthesis could not be reproduced. The XRD data show that both the "grass" and the "tangle" morphologies consist of type II red phosphorus, most clearly shown by the shape of the peaks around $2\theta = 16°$. The presence of a peak at 16.4° and the absence at 19.8° rules out type III red phosphorus.[5]

Raman spectroscopy provides complementary structural evidence (Figure 5b). Although the Raman spectra for black, Hittorf's, white, and various samples of amorphous red phosphorus are known,[1,21,22] good Raman spectra of the other crystalline forms of red phosphorus are not freely available. The Raman spectra of black phosphorus, fibrous red phosphorus and type II red phosphorus were collected for comparison with the new phosphorus nanostructures. The

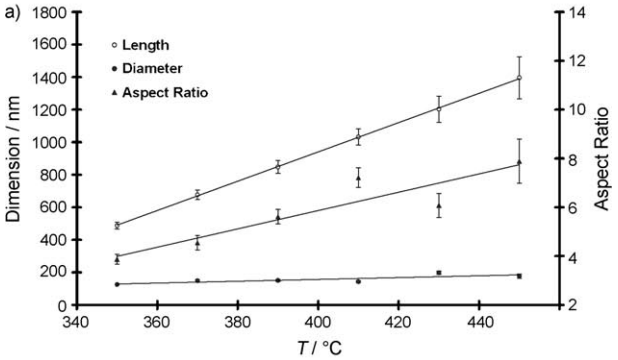

SAED spot	Corresponding spacing	Comparison with powder data of "type II" red phosphorus
●	5.67 (±0.02) Å	5.66 Å
○	5.41 (±0.02) Å	5.39 Å
▲	3.06 (±0.02) Å	3.08 Å
△	2.82 (±0.01) Å	2.82 Å
×	2.63 (±0.01) Å	2.62 Å

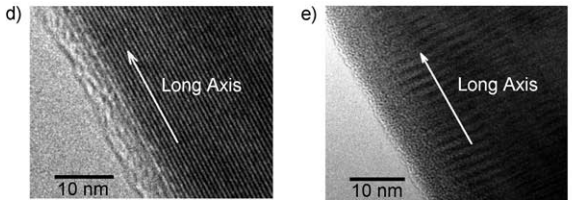

Figure 4. a) Plot of the mean dimensions of the "grass" nanorods, as a function of synthesis temperature (mean of 30–70 rods per data point); b) TEM image showing a typical nanorod from a 400 °C synthesis. Inset: EDS spectrum and electron diffraction pattern; c) summary of the diffraction pattern shown in (b), with analysis of the corresponding lattice spacings; d) and e) HRTEM images showing lattice spacings of 5.7 Å and 18.3 Å, parallel and perpendicular, respectively, to the nanorod long axis, and a surface (probably oxide) coating.

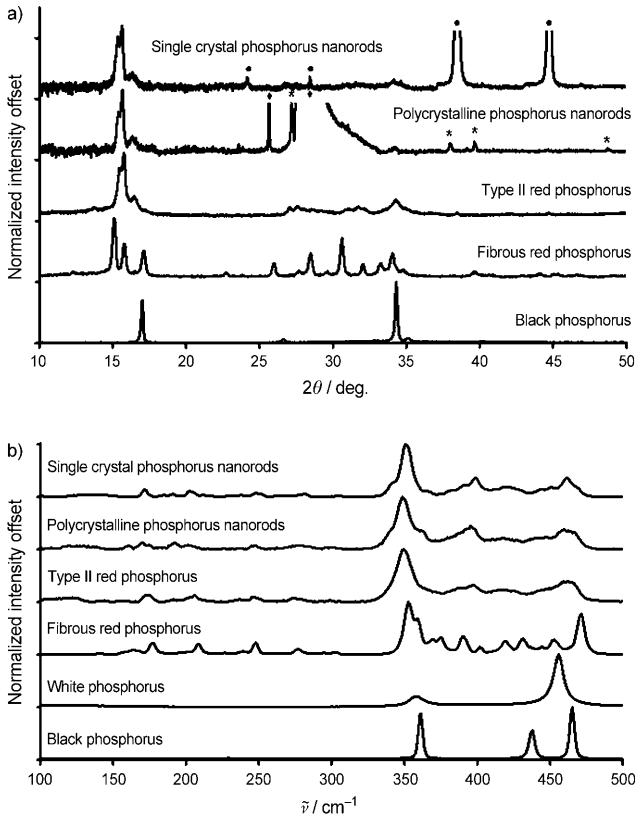

Figure 5. a) Powder X-ray diffraction patterns of the new phosphorus nanostructures alongside control spectra for type II red, fibrous red, and black phosphorus. Peaks arising from the alumina sample holder are annotated with filled circles (●) in the data for single-crystal phosphorus nanorods. In the case of the polycrystalline phosphorus nanorods, the peaks at 25.7° and 28.4° (labeled ◆) are features of the scrubbed silicon substrate, whereas the peaks annotated with asterisks (*) match the diffraction pattern of rhombohedral bismuth; b) Raman spectra of the new phosphorus structures alongside control spectra for type II red, fibrous red, white, and black phosphorus, for comparison.

spectra suggested that both varieties of nanorod consist of type II red phosphorus, although the nanorods showed additional and distinct features, particularly around 350 and 460 cm^{-1}.

In summary, we have shown that nanorods of elemental phosphorus can be synthesized using a simple, ampoule-based technique. Bismuth nanoparticles, formed in situ, catalyze VLS growth of polycrystalline phosphorus nanorods with diameters on the order of 100 nm and lengths of several microns. Single-crystal phosphorus nanorods, with diameters of approximately 160 nm and lengths which are systematically controlled by synthesis temperature, are formed under similar conditions in the absence of metal catalyst. Tantalizing evidence also suggests that tubular nanostructures of phosphorus may be synthesized, although oxidized nanorods rendered hollow by Kirkendall effects cannot be ruled out.[23] Further experimental work is underway to explore the physical and electronic characteristics of the various products relevant to potential applications. A combination of SAED studies on the single-crystal nanorod product and theoretical studies will allow determination of the crystal structure of type II red phosphorus.

Experimental Section

Typical synthetic procedure: White phosphorus (0.05 g, 0.4 mmol; see the Supporting Information, section 1 for purification details) was placed in a test tube (internal diameter 8 mm) in an argon atmosphere (Pureshield, 99.995%), and held in place with a small plug of glass wool. Bismuth (0.1 g, 0.05 mmol; Alfa Aesar 12208, 99.99%) was mechanically pulverized and dusted onto the (111) surface of a small (0.5–0.8 cm^2) silicon wafer. After loading the bismuth-coated wafer, the test tube was sealed with a propane–oxygen flame under flowing argon, to produce an ampoule 4–5 cm long (Figure 1a and b). The ampoule was placed inside a stainless steel protective bomb and heated in a muffle furnace to the required synthesis temperature for between 4 and 18 h. The ampoules were broken open in an argon filled glove box running at $< 0.1\%$ oxygen.

Samples for SEM (LEO Gemini FEGSEM, 5 kV) were prepared by attaching the silicon wafer from the ampoule directly onto an SEM puck with conductive carbon tape. Exposure to air occurred for a short period (approximately ten minutes) whilst the samples were loaded into the SEM. Samples for TEM were prepared by placing reacted wafers in a small quantity of degassed ethanol (VWR International, 99.7%), bath-sonicating for two minutes, and then drying a drop of the resulting suspension onto a holey carbon film coated TEM grid. Air exposure occurred for up to 24 h, between sample preparation and loading into the TEM. TEM examination was carried out on JEOL 2000 and JEOL 2010 microscopes (the latter for high resolution work), both operating at 200 kV. (Micro)Raman spectroscopy was carried out on a Horiba Infinity spectrometer using a red 628 nm laser, by focusing on the relevant region.

The XRD patterns for black phosphorus and fibrous red phosphorus were measured using a PW1710 (Phillips, Amsterdam, Netherlands) diffractometer, using $Cu_{K\alpha}$ radiation with $\lambda = 1.5406$ Å. Samples were prepared by dispersing finely ground powders of the materials onto a silicon sample holder. The XRD patterns for type II red phosphorus, single-crystal phosphorus nanorods, and polycrystalline phosphorus nanorods were measured on an X'Pert PRO X-ray diffractometer fitted with an X'Celerator RTMS detector (Phillips, Amsterdam, Netherlands), also using $Cu_{K\alpha}$ radiation. Samples of type II red phosphorus and single crystal phosphorus nanorods were prepared by dispersing finely ground powders of each material onto an aluminum sample holder. The polycrystalline nanorod sample was prepared by attaching a silicon wafer from a reacted ampoule onto a sample holder with adhesive putty.

Received: October 24, 2008
Revised: December 15, 2008
Published online: January 29, 2009

Keywords: allotropy · bismuth · electron microscopy · nanostructures · phosphorus

[1] H. Ostmark, S Wallin, N. Hore, O. Launila, *J. Chem. Phys.* **2003**, *119*, 5918–5922.
[2] a) A. Brown, S. Rundqvist, *Acta Crystallogr.* **1965**, *19*, 684–685; b) S. Lange, P. Schmidt, T. Nilges, *Inorg. Chem.* **2007**, *46*, 4028–4035.
[3] A. Pfitzner, *Angew. Chem.* **2006**, *118*, 714–715; *Angew. Chem. Int. Ed.* **2006**, *45*, 699–700.
[4] D. E. C. Corbridge, *The Structural Chemistry of Phosphorus*, Elsevier Scientific Publishing Company, Amsterdam, **1974**, pp. 13–24.

[5] W. L. Roth, T. W. DeWitt, A. J. Smith, *J. Am. Chem. Soc.* **1947**, *69*, 2881 – 2885.
[6] M. Ruck, D. Hoppe, B. Wahl, P. Simon, Y. Wang, G. Seifert, *Angew. Chem.* **2005**, *117*, 7788 – 7792; *Angew. Chem. Int. Ed.* **2005**, *44*, 7616 – 7619.
[7] W. Hittorf, *Ann. Phys. Chem.* **1865**, *126*, 193.
[8] a) M. Haeser, S. Bocker, *Z. Anorg. Allg. Chem.* **1995**, *621*, 258 – 286; b) M. Haser, *J. Am. Chem. Soc.* **1994**, *116*, 6925 – 6926.
[9] a) A. Pfitzner, *Chem. Eur. J.* **2000**, *6*, 1891 – 1898; b) H. M. Moller, W. Jeitschko, *J. Solid State Chem.* **1986**, *65*, 178 – 189; c) A. Pfitzner, E. Freudenthaler, *Angew. Chem.* **1995**, *107*, 1784 – 1786; *Angew. Chem. Int. Ed. Engl.* **1995**, *34*, 1647 – 1649; d) A. Pfitzner, E. Freudenthaler, *Z. Naturforsch. B* **1997**, *52*, 199 – 202.
[10] A. Pfitzner, M. F. Brau, J. Zweck, G. Brunklaus, H. Eckert, *Angew. Chem.* **2004**, *116*, 4324 – 4327; *Angew. Chem. Int. Ed.* **2004**, *43*, 4228 – 4231.
[11] A. J. Karttunen, M. Linnolahti, T. A. Pakkanen, *Chem. Eur. J.* **2007**, *13*, 5232 – 5237.
[12] W. Lu, C. M. Lieber, *Nat. Mater.* **2007**, *6*, 841 – 850.
[13] F. Hussain, M. Hajjati, M. Okamoto, R. E. Gorga, *J. Compos. Mater.* **2006**, *40*, 1511 – 1575.
[14] I. Cabria, J. W. Mintmire, *Europhys. Lett.* **2004**, *65*, 82 – 88.
[15] G. Seifert, E. Hernandez, *Chem. Phys. Lett.* **2000**, *318*, 355 – 360.
[16] A. Morita, *Appl. Phys. A* **1986**, *39*, 227 – 242.
[17] R. S. Wagner, W. C. Ellis, *Appl. Phys. Lett.* **1964**, *4*, 89 – 90.
[18] Y. Ando, X. Zhau, T. Sugai, M. Kumar, *Mater. Today* **2004**, *7*, 22 – 49.
[19] Y. Y. Wu, P. D. Yang, *J. Am. Chem. Soc.* **2001**, *123*, 3165 – 3166.
[20] L. Wang, Z. Cui, Z. Zhang, *Surf. Coat. Technol.* **2007**, *201*, 5330 – 5332.
[21] S. Sugai, T. Ueda, K. Murase, *J. Phys. Soc. Jpn.* **1981**, *50*, 3356 – 3361.
[22] D. J. Olego, J. A. Baumann, R. Schachter, *Solid State Commun.* **1985**, *53*, 905 – 908.
[23] a) J. H. Fan, M. Knez, R. Scholz, K. Nielsch, E. Pippel, D. Hesse, M. Zacharias, U. Gosele, *Nat. Mater.* **2006**, *5*, 627 – 631; b) Y. Yin, R. M. Rioux, C. K. Erdonmez, S. Hughes, G. A. Somorjiai, A. P. Alivisatos, *Science* **2004**, *304*, 711 – 714.

